

BASIC RESEARCH

Effects of recombinant human canstatin protein in the treatment of pancreatic cancer

Xiao-Ping He, Zhao-Shen Li, Ren-Min Zhu, Zhen-Xing Tu, Jun Gao, Xue Pan, Yan-Fang Gong, Jing Jin, Xiao-Hua Man, Hong-Yu Wu, Ai-Fang Xu

Xiao-Ping He, Ren-Min Zhu, Department of Gastroenterology, Nanjing General Hospital, Nanjing 210002, Jiangsu Province, China

Zhao-Shen Li, Zhen-Xing Tu, Jun Gao, Xue Pan, Yan-Fang Gong, Jing Jin, Xiao-Hua Man, Hong-Yu Wu, Ai-Fang Xu, Department of Gastroenterology, the Affiliated Changhai Hospital of Second Military Medical University, Shanghai 200433, China

Supported by the Major Basic Research Programs of Shanghai Science and Technology Commission, No. 03JC14007

Correspondence to: Zhao-Shen Li, MD, Director of Gastroenterology Department, Changhai Hospital, Shanghai 200433, China. lzs@126.com

Telephone: +86-21-25070552

Received: 2006-07-18

Accepted: 2006-09-13

Abstract

AIM: To examine the effect of canstatin, a newly discovered endogenous inhibitor of angiogenesis, in the treatment of pancreatic cancer *in vivo*.

METHODS: The canstatin cDNA fragment was synthesized and amplified from the total RNA extracted from human placenta tissues by RT-PCR. The resulting product was firstly cloned into pUCm-T vector, then into plasmid pET-22b (+) and transformed into *E. coli* BL21. Isopropyl-1-thio- β -Dgalactopyran-oside (IPTG) was used to induce the expression of canstatin protein and affinity chromatography was used to purify the protein. To determine the activity of purified recombinant human canstatin (rhCanstatin), orthotopic xenograft human pancreatic cancer models were established. Human pancreatic cancer cells (SW1990) were injected into the pancreas of BALB/c nude mice. Twenty-four nude mice with orthotopic xenograft tumor were randomly divided into 3 groups 10 d after the inoculation, and were treated with PBS 0.3 mL, or canstatin 5 mg/kg, or 10 mg/kg per day for 3 wk intraperitoneally. When the experiment was over, all tumors were resected and the effects of rhCanstatin on tumor growth, microvessel density (MVD) were analyzed.

RESULTS: After IPTG induction, SDS-PAGE showed a new monomeric 24 kDa protein band. This protein was purified through affinity chromatography and refolded through dialysis with a final concentration of 60 mg/L. In orthotopic pancreatic cancer models, the final tumor volume in groups treated with PBS, canstatin 5 mg/kg, 10 mg/kg were $355.21 \pm 39.54 \text{ mm}^3$, $112.73 \pm$

10.47 mm^3 , and $61.75 \pm 6.99 \text{ mm}^3$ respectively. The immunohistochemical examination showed that the MVD in tumors treated with canstatin was significantly less than that in other group.

CONCLUSION: These findings demonstrate that the rhCanstatin effectively retards the growth of pancreatic cancer in a dose-dependent manner through inhibiting angiogenesis and may be a promising therapeutic agent for pancreatic cancer treatment in the clinic.

© 2006 The WJG Press. All rights reserved.

Key words: Canstatin; Angiogenesis; Pancreatic cancer; Anti-tumor agent

He XP, Li ZS, Zhu RM, Tu ZX, Gao J, Pan X, Gong YF, Jin J, Man XH, Wu HY, Xu AF. Effects of recombinant human canstatin protein in treatment of pancreatic cancer. *World J Gastroenterol* 2006; 12(41): 6652-6657

<http://www.wjgnet.com/1007-9327/12/6652.asp>

INTRODUCTION

The prognosis of patients with pancreatic cancer is poor, with or without treatment. The American National Cancer Institute (NCI) reported in its SEER Cancer Statistics Review that there are approximately 27 000 new cases of pancreatic cancer, resulting in around 26 000 deaths each year in the US. It is now the fourth most common cause of cancer deaths in USA and among the top ten common causes of cancer deaths in China. Being extremely aggressive, pancreatic cancer is often far advanced by the time symptoms occur, and a definitive diagnosis is established, with less than 20% resectable chance. The total 5-year survival rate is less than 5% from the time of diagnosis, although combination therapy has been accepted using radiation therapy or chemotherapy with or without surgery. Therefore, it is urgent to develop new treatment strategy for this malignant disease.

Angiogenesis, the formation of new capillary blood vessels, plays an essential role in normal and pathological processes, such as embryogenesis, wound healing and tumor growth^[1-2]. Angiogenesis is also essential for the growth of solid tumors and their metastases^[3-4]. Solid tumors cannot grow beyond a few millimeters in diameter

without generation of tumor vasculature. Furthermore, the denser the blood vessel formation, the higher the rate of tumor growth and the greater the metastatic potential^[5]. Extensive research has led to the identification and isolation of several regulators of angiogenesis, some of which represent therapeutic targets.

Canstatin, a 24-kDa NC1 domain of the α_2 chain of type IV collagen, is a newly discovered endogenous inhibitor of angiogenesis following the discovery of endostatin^[6,7]. Previous studies have shown that canstatin efficiently suppresses the growth of human prostate carcinoma and renal cell carcinoma in models, even more potent than endostatin^[8]. However, it is still unknown whether canstatin is effective in the treatment of pancreatic cancer. In this study, we cloned canstatin DNA sequence, expressed and purified recombinant human canstatin (rhCanstatin) and detected its anti-tumor effects on pancreatic cancer.

MATERIALS AND METHODS

Vectors, host bacteria and reagents

E. coli DH5 α was preserved in our laboratory. *E. coli* BL21 and plasmid expression vector pET-22b (+) were purchased from the College of Life Sciences of Fudan University. pUCm-T vector was purchased from Shenergy Biocolor. *Bam*HI, *Hind*III, T4 DNA ligase and DNA molecular weight marker were supplied by New England Biolabs. Protein marker was purchased from Shanghai Sangon Co. Trizol was provided by Jingmei Biotech. One-step reverse transcription polymerase chain reaction (RT-PCR) kit was purchased from Takara. Isopropyl-1-thio- β -D-galactopyranoside (IPTG), X-gal, plasmid mini kit, gel extraction mini kit and Coomassie Brilliant Blue R250 were purchased from Shanghai Watson. Nickelnitrilotriacetic acid-agarose column was purchased from Qiagen. The placental tissues were kindly provided by a woman who underwent caesarean operation in our hospital with informed consent. A pair of gene specific primers was designed according to canstatin DNA sequence presented in GenBank.

The forward primer (5'-CGGGATCCTGTCAGCATCGCTACCTC-3') and reverse primer (5'-CCCAAGCTTCAGGTCTTCATGCACAC-3') were synthesized by Shanghai Sangon.

Cell line, animals and antibody

A human pancreatic cancer cell line SW1990 was preserved in our laboratory. Cells were maintained in culture in DMEM supplemented with 10% fetal bovine serum (FBS) and antibiotics (100 units/mL penicillin and 100 μ g/mL streptomycin). BALB/c male nude mice were purchased from Institute of Animal Center of Chinese Academy of Sciences in Shanghai. Rat anti-mouse CD34 monoclonal antibody was purchased from Hbt Biotechnology.

RNA isolation

The fresh human placental tissues were frozen in liquid nitrogen immediately after dissection. The total RNA was isolated from the tissues using trizol according to the

instruction. Pellets of the total RNA were dissolved in diethyl pyrocarbonate-treated water and finally quantitated by measurement of the optical density at 260 nm through spectrophotometer and stored at -80°C before use.

Amplification of target sequences by RT-PCR

The sequence encoding canstatin was amplified by RT-PCR from the total RNA. RT-PCR was performed in a 50 μ L of reaction system containing 10 \times reaction buffer (5 μ L), 25 mmol/L MgCl₂ (10 μ L), 10 mmol/L mixture of four dNTPs (5 μ L), 40 MU/L ribonucleases inhibitor 1 μ L, 5 MU/L AMV reverse transcriptase XL (1 μ L), 5 MU/L AMV-Optimized Taq DNA polymerase (1 μ L), 25 μ mol/L forward primer (1 μ L), 25 μ mol/L reverse primer (1 μ L), 1.8 g/L total RNA template (1 μ L), ribonucleases free double distilled H₂O (24 μ L). RT-PCR conditions were: reverse transcription reaction at 50°C for 40 min, initial denaturation at 94°C for 2 min, 35 cycles, each cycle consisting of denaturation at 94°C for 40 s, annealing at 52.6°C for 40 s and extension at 72°C for 1 min, and after the cycles a final extension at 72°C for 5 min. The RT-PCR products were added to 6 \times loading buffer, mixed and run on 1% agarose gel (0.5 μ g/mL ethidium bromide). After electrophoresis at 100 volts for 40 min, the gel was examined under ultraviolet light and photographed. The PCR products were recovered from the gel following the instruction of gel extraction mini kit.

Cloning of the PCR products

The ligation mixture included 10 \times ligation buffer 1 μ L, pUCm-T 1.5 μ L, purified PCR products 6.5 μ L and T4 DNA ligase 1 μ L. After incubated overnight at 16°C, 3 μ L of the ligation reactions was used to transform the competent *E. coli* DH5 α by electroporation. The transformed cells were gently spread over the surface of the agar plate covered with IPTG and X-gal and containing appropriate ampicillin. The plate was inverted and incubated overnight at 37°C.

Identification of bacterial colonies containing recombinant plasmids

Six white single bacterial colonies were picked from the agar plate and then inoculated into different LB medium containing ampicillin with the final concentration of 100 mg/L. The cultures were incubated overnight at 37°C with vigorous shaking. Plasmid DNAs were isolated from each culture by the alkaline lysis method presented in the kit and then analyzed by gel electrophoresis after digestion with *Bam*HI or *Hind*III.

DNA sequencing

The positive colony was sequenced on both strands with universal primers M13-/T7 by the Sanger Dideoxy-mediated chain-termination method. The nucleotide sequence was compared with that in GenBank database.

Construction of prokaryotic expression vector

The recombinant plasmid DNAs were extracted by the method described earlier, digested with both *Bam*HI and *Hind*III, and finally ligated into predigested pET22b

vector by T4 DNA ligase. Plasmid constructs encoding canstatin were transformed into *E. coli* BL21 through electroporation. The transformed cells were gently spread over the surface of the agar plate containing ampicillin and incubated overnight at 37°C. Seven white single bacterial colonies were picked from the agar plate and grown in small-scale LB medium containing 100 mg/L ampicillin. Plasmid DNAs were isolated from each culture and restriction analysis was performed.

Expression of rhCanstatin

An overnight bacterial culture was used to inoculate a 200-mL culture into LB medium. This culture was grown for approximately 3.5 h until the cells reached an A600 of 0.6. Then, protein expression was induced by addition of IPTG to a final concentration of 0.5 mmol/L. After a 3-h induction, cells were harvested by centrifugation at $12\,000 \times g$. The expression level of the protein was assessed by analysis on 12% SDS-PAGE gel followed by staining of Coomassie Brilliant Blue R250.

Purification and refolding of rhCanstatin

The harvested cells were suspended in 1 mmol/L EDTA, 0.1 mol/L NaCl, 0.05 mol/L Tris-HCl, pH 8.0, sonicated briefly and centrifuged at 5000 g for 20 min at 4°C. The precipitated fraction was washed by 10 mL of 5 mmol/L imidazole, 0.5 mol/L NaCl, 0.02 mol/L Tris-HCl, pH 7.5 and again centrifuged at 5000 g for 20 min at 4°C. The supernatant fraction was discarded. The sediment was lysed in 8 mol/L urea, 0.5 mol/L NaCl, 0.02 mol/L Tris-HCl, pH 7.9 and passed over a 5-mL of nickelnitrilotriacetic acid-agarose column which had been equilibrated and washed with buffer 0 (8 mol/L urea, 0.5 mol/L NaCl, 0.02 mol/L Tris-HCl, pH 8.0) at a speed of 2 mL/min. The column was then stepwisely eluted by 15 mL each of 10, 25, 50, 125 and 250 mmol/L imidazole in buffer 0. The eluted fraction was collected separately and analyzed on SDS-PAGE gel. The eluted protein between 125 and 250 mmol/L imidazole was dialyzed three times against 2 liters of PBS at 4°C. Protein concentration was determined by the BCA assay.

In vivo tumor studies

Human pancreatic adenocarcinoma cells (SW 1990) were harvested from culture, and 1×10^7 cells in sterile PBS were injected into the pancreas of 4-wk-old male BALB/c nude mice. The tumors grew for 10 d, after which animals were divided into groups of 8 mice each and treated with PBS 0.3 mL, or canstatin 5 mg/kg, or 10 mg/kg per day for 3 wk. All agents were injected intraperitoneally. When the experiment was over, all tumors were resected. Tumor length and width were measured using a Vernier caliper, and the tumor volume was calculated using the standard formula: length \times width squared \times 0.5.

CD34 immunohistochemistry

At the end of treatment, mice were sacrificed, and the tumors were excised. The removed tumors were dissected with a scalpel into several pieces approximately 3-4 mm thick and then fixed in 4% paraformaldehyde for 24 h.

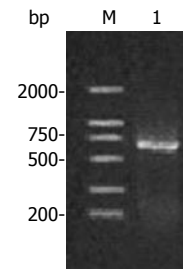


Figure 1 Amplification products of human canstatin. Lane M: DNA marker; Lane 1: RT-PCR products.

Tissues were then transferred to PBS for 24 h before dehydration and paraffin embedding. After embedding in paraffin, 3-mm tissue sections were sliced and mounted. Sections were deparaffinized, rehydrated, and blocked with 10% rabbit serum. Next, slides were incubated at 4°C overnight with a 1:50 dilution of rat anti-mouse CD34 monoclonal antibody, followed by two successive incubations at 37°C for 30 min with 1:50 dilutions of biotin-conjugated secondary antibodies and HRP-conjugated streptavidin. Finally, diaminobenzidine was used as the chromogen. All slides were counterstained with Meyer's hematoxylin and observed under light microscope. Microvessel areas were quantified by manual counting of hotspots in sections, as described by Weidner *et al*^[9].

Statistical analysis

Results were expressed as mean \pm SE. Unpaired *t* test was used to compare different groups of data as indicated. A 2-tailed *P* value of < 0.05 was considered significant.

RESULTS

Amplification of target sequences

The extracted total RNA was separated into three clear bands indicating 28S, 18S, and 5S after agarose gel electrophoresis. When the sample was diluted 50 times by diethyl pyrocarbonate-treated water, the values of A_{260} and A_{280} were 0.879 and 0.410 respectively with a $A_{260}:A_{280}$ ratio 2.095 through spectrophotometer. So the concentration of total RNA was 1.8 g/L according to the equation: total RNA concentration = $40 \times A_{260} \times \text{dilution power}/1000$. The target sequences were specifically amplified through RT-PCR, showing a clear band near the location of 684 bp DNA on agarose gel (Figure 1).

Cloning in plasmid vectors and identification of bacterial colonies

After recovered from the gel, the resulting RT-PCR products were ligated into pUCm-T vectors, and the pUCm-T/canstatin constructs were then transformed into *E. coli* DH5 α . Both blue and white colonies appeared on the agar plate after an overnight incubation. Six white colonies were selected. Restriction analysis of small-scale preparations of plasmid DNAs showed the plasmid DNAs in one white colony were separated into two bands near the locations of primary plasmid and objective gene fragment after digested by *Hind*III but only one band near

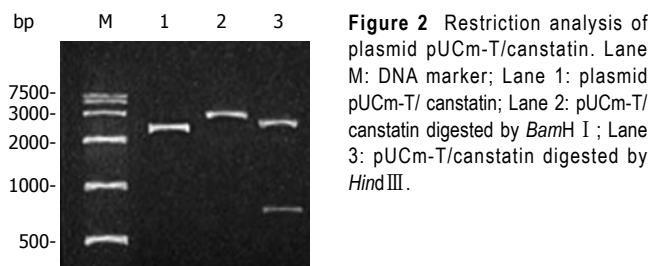


Figure 2 Restriction analysis of plasmid pUCm-T/canstatin. Lane M: DNA marker; Lane 1: plasmid pUCm-T/canstatin; Lane 2: pUCm-T/canstatin digested by *Bam*HI; Lane 3: pUCm-T/canstatin digested by *Hind*III.

the location of primary plasmid after digested by *Bam*HI (Figure 2). DNA sequencing demonstrated the sequence of this cloned gene was completely homologous to the canstatin gene sequence represented in GenBank.

Construction and identification of prokaryotic expression vector

The canstatin cDNA was cut down from pUCm-T with *Bam*HI and *Hind*III and ligated into the vector pET-22b (+). The resultant plasmid pET-22b (+)/canstatin was then transformed into *E. coli* BL21. White colonies appeared on LB agar plate after an overnight incubation. Seven of them were picked and restriction analysis showed the plasmids DNA of all selected colonies were separated into two specific bands, one of which was the objective gene fragment (Figure 3).

Expression and purification of rhCanstatin

After IPTG induction, SDS-PAGE analysis revealed a monomeric band at about 24 kDa. The relative quantitative values of expressed products over total bacterial proteins after 3 h of induction were 16.8 with the percentage of total protein 23.0% estimated by densitometry using Quantity One 4.1.1 protein analysis software (Figure 4). RhCanstatin was eluted from the column with two concentrations of imidazole (125 and 250 mmol/L). The concentration of dialyzed rhCanstatin was 60 mg/L.

In vivo tumor experiments

Established orthotopic xenograft tumor models in mice were used to test the effectiveness of canstatin as an inhibitor of angiogenesis-dependent tumor growth. The final tumor volumes in groups treated with PBS, canstatin 5 mg/kg and canstatin 10 mg/kg were $355.21 \pm 39.54 \text{ mm}^3$, $112.73 \pm 10.47 \text{ mm}^3$, and $61.75 \pm 6.99 \text{ mm}^3$ respectively (Figure 5A), and the tumor weights were $0.64 \pm 0.08 \text{ g}$, $0.21 \pm 0.02 \text{ g}$, and $0.12 \pm 0.02 \text{ g}$ respectively. The immunohistochemical examination showed that the MVD in tumors treated with canstatin 5 mg/kg (27.4 ± 6.1) or 10 mg/kg (20.2 ± 4.1) was significantly less than that in PBS group (40.2 ± 7.4) (Figure 5B). This decrease in tumor size was consistent with a decrease in CD34-positive vasculature (Figure 5C and D). In all of the *in vivo* studies, mice appeared healthy with no signs of wasting, and none of the mice died during treatment.

DISCUSSION

Pancreatic cancer is a major cause of morbidity and mortality worldwide. It is an extremely life-threatening

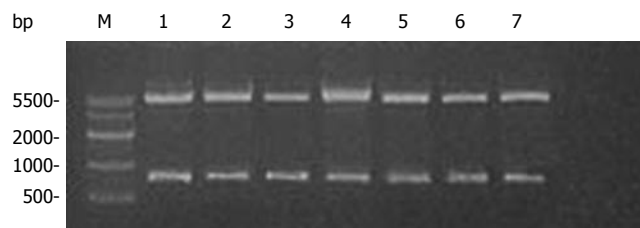


Figure 3 Restriction analysis of plasmid pET-22b(+)/canstatin. Lane M: DNA marker; Lanes 1 to 7: plasmid DNAs of seven selected colonies digested by both *Bam*HI and *Hind*III.

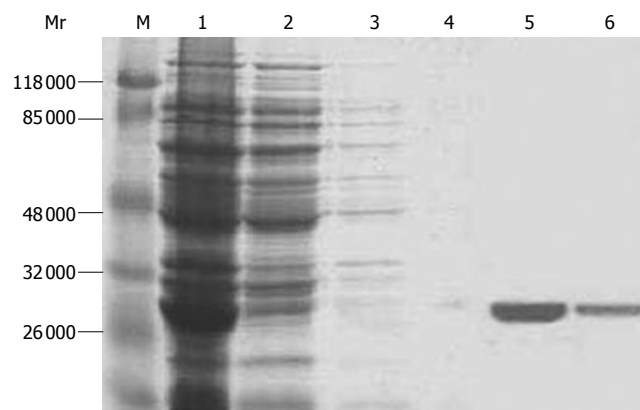


Figure 4 SDS-PAGE gel electrophoresis of purified protein. Lane M: protein marker; lane 1: total bacterial protein; lane 2: 10 mmol/L imidazole elution; lane 3: 25 mmol/L imidazole elution; lane 4: 50 mmol/L imidazole elution; lane 5: 125 mmol/L imidazole elution; lane 6: 250 mmol/L imidazole elution.

neoplasm due to its late diagnosis, rapid progression and resistance to chemo- and radiotherapy. Statistics data show it is the fourth leading cause of cancer death in the USA, with a median survival of less than 6 mo, and a 5-year survival rate of less than 5%^[10,11]. Despite the great improvements in conventional therapy, including surgery, chemotherapy and radiotherapy, the mortality of this disease remains almost unchanged. There is, therefore, an urgent need for novel treatment strategies for this deadly disease.

Antiangiogenesis therapy is a new and attractive target for tumor therapy. By interrupting new vessel formation, tumor growth can be effectively arrested^[12-16]. Compared to conventional therapy such as chemotherapy, antiangiogenesis has several advantages theoretically^[17,18]. Firstly, it has lower toxicity. Second, tumor vasculature is less mature and more sensitive to inhibiting agents than normal vessels. Third, due to the low mutagenesis rate of normal cell type, the endothelial cell is less likely to counteract therapeutic drugs through development of multi-drug resistance mechanisms. Fourth, drugs have easy access to their therapeutic target. In antiangiogenic therapy the target cells are those which constitute vessel walls, so intravenous antiangiogenic agents act on these cells directly. Fifth, antiangiogenic therapy has an inherent 'amplification' mechanism. Successful interference with only a few endothelial cells may lead to disruption of a whole vessel. Loss of a single vessel may deprive a significant number of tumor cells of essential nutrients, leading to cell death.

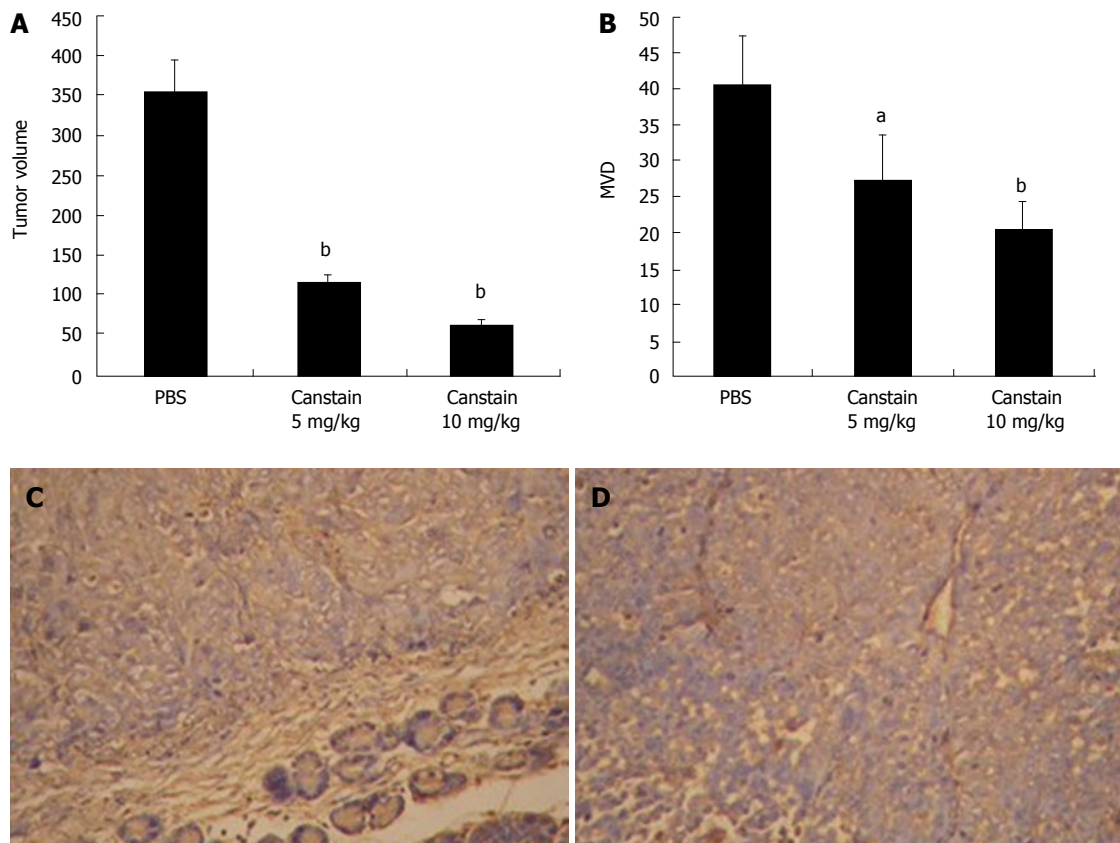


Figure 5 *In vivo* antitumor effects in a xenograft model. The *in vivo* antitumor effect of the canstatin was analyzed in a SW1990 human pancreatic cancer cell orthotopic xenograft model. **A:** Tumor volumes in different groups: Canstain 5 mg/kg or 10 mg/kg treatment showed a significantly stronger anti-tumor effect, compared with the PBS treated group (^a $P < 0.01$); **B:** MVD in xenograft models: significant inhibition of angiogenesis was observed in groups treated with canstain 5 mg/kg or 10 mg/kg compared with that in the control group (^a $P < 0.05$, ^b $P < 0.01$, respectively); **C:** CD34 immunohistochemistry in group treated with PBS ($\times 200$): tumor sections showed extensive angiogenesis; **D:** CD34 immunohistochemistry in group treated with canstain ($\times 200$): tumor sections showed obviously decreased new vessels with a small focus of necrosis.

In light of these, this new therapy concept has aroused much attention and fueled the development of novel anti-angiogenic agents.

Despite some initial setbacks and negative clinical trial results, major progress has been made over the past few years in targeting angiogenesis for human cancer therapy. In Feb 2004, the US Food and Drug Administration (FDA) approved bevacizumab, a humanized anti-VEGF (vascular endothelial growth factor) monoclonal antibody, for the treatment of metastatic colorectal cancer, following a phase III study showing a survival benefit^[19]. In Dec 2004, the FDA approved pegaptinib, an aptamer that blocks the 165 amino-acid isoform of VEGF-A, for the treatment of the wet (neovascular) form of age-related macular degeneration (AMD)^[20]. Angiogenesis inhibitors for the treatment of cancer have now been approved by the FDA in the US and in 28 other countries, including the European Union. When Avastin was approved in the US, Mark McClellan, the Director of the FDA, stated that: "Angiogenesis inhibitors can now be considered as the fourth modality of cancer therapy."

Canstain, derived from the C-terminal globular non-collagenous (NC1) domain of the α_2 chain of type IV collagen, is a new endogenous inhibitor of angiogenesis, which has been shown to successfully suppress the growth of implanted human prostate carcinoma and renal cell

carcinoma in mice, even more potent than endostatin^[21,22].

In the present study, placental tissues with abundant vessels were chosen to extract total RNA. And we successfully constructed a prokaryotic expression system to express rhCanstain protein. *E. coli* was used as host bacteria because of its ability of rapid growth, well-characterized genetic background, high expression level, and cheapness, which is considered as the most attractive and ideal system for heterologous protein expression. The pET-22b (+) vector, as the expression vector, carries an N-terminal pelB signal sequence plus C-terminal His-Tag[®] sequence^[23,24]. In our study, the resulting cDNA fragment was digested with *Bam*HI and *Hind*III and ligated into predigested pET-22b (+). This placed canstain downstream of and in-frame with the pelB leader sequence, allowing for periplasmic localization and expression of soluble protein. The 3' end of the sequence was ligated in-frame with the polyhistidine tag sequence which also facilitated the purification of this target protein. After IPTG induction, SDS-PAGE analysis revealed a 24 kDa monomeric band, demonstrating the successful expression of target protein. Through affinity chromatography and dialysis, the production of rhCanstain was purified and refolded with a final concentration of 60 mg/L and chick chorioallantoic membrane (CAM) assay demonstrated that rhCanstain successfully inhibited newly formed blood

vessels in a dose-dependent manner.

Moreover, *in vivo* experiments showed that rhCanstatin successfully inhibited the growth of human pancreatic tumors by 3.15 fold or 5.75 fold at the dose of 5 mg/kg or 10 mg/kg respectively compared with placebo-treated mice. And this decrease in tumor size was consistent with a decrease in CD34-positive vasculature. Our findings demonstrate that rhCanstatin suppressed the growth of pancreatic cancer through inhibition of angiogenesis in a dose-dependent manner and suggest it may be a new potent anti-tumor agent for these patients. These findings add meaningful information to our understanding of the biological activity of rhCanstatin.

In conclusion, our findings verify the viewpoint that angiogenesis is an important target for cancer therapy. Animal tumor experiments demonstrate that the soluble rhCanstatin with antiangiogenic activity is a potential agent for pancreatic cancer therapy. It is meaningful to explore the applications of rhCanstatin in clinical use and study how to achieve the most effective combinations of antiangiogenic agents with chemotherapy or other biological agents in future.

REFERENCES

- Carmeliet P.** Angiogenesis in life, disease and medicine. *Nature* 2005; **438**: 932-936
- Greenberg DA, Jin K.** From angiogenesis to neuropathology. *Nature* 2005; **438**: 954-959
- Dudek AZ, Pawlak WZ, Kirstein MN.** Molecular targets in the inhibition of angiogenesis. *Expert Opin Ther Targets* 2003; **7**: 527-541
- Fishman M, Antonia S.** Novel therapies for renal cell carcinoma-an update. *Expert Opin Investig Drugs* 2003; **12**: 593-609
- Wang ZQ, Li JS, Lu GM, Zhang XH, Chen ZQ, Meng K.** Correlation of CT enhancement, tumor angiogenesis and pathologic grading of pancreatic carcinoma. *World J Gastroenterol* 2003; **9**: 2100-2104
- Kalluri R.** Basement membranes: structure, assembly and role in tumour angiogenesis. *Nat Rev Cancer* 2003; **3**: 422-433
- Folkman J.** Antiangiogenesis in cancer therapy--endostatin and its mechanisms of action. *Exp Cell Res* 2006; **312**: 594-607
- Kamphaus GD, Colorado PC, Panka DJ, Hopfer H, Ramchandran R, Torre A, Maeshima Y, Mier JW, Sukhatme VP, Kalluri R.** Canstatin, a novel matrix-derived inhibitor of angiogenesis and tumor growth. *J Biol Chem* 2000; **275**: 1209-1215
- Weidner N, Gasparini G.** Determination of epidermal growth factor receptor provides additional prognostic information to measuring tumor angiogenesis in breast carcinoma patients. *Breast Cancer Res Treat* 1994; **29**: 97-107
- Takhar AS, Palaniappan P, Dhingsa R, Lobo DN.** Recent developments in diagnosis of pancreatic cancer. *BMJ* 2004; **329**: 668-673
- Qiu D, Kurosawa M, Lin Y, Inaba Y, Matsuba T, Kikuchi S, Yagyu K, Motohashi Y, Tamakoshi A.** Overview of the epidemiology of pancreatic cancer focusing on the JACC Study. *J Epidemiol* 2005; **15** Suppl 2: S157-S167
- Morioka H, Weissbach L, Vogel T, Nielsen GP, Faircloth GT, Shao L, Hornicek FJ.** Antiangiogenesis treatment combined with chemotherapy produces chondrosarcoma necrosis. *Clin Cancer Res* 2003; **9**: 1211-1217
- Camp-Sorrell D.** Antiangiogenesis: the fifth cancer treatment modality? *Oncol Nurs Forum* 2003; **30**: 934-944
- Qin RY, Fang RL, Gupta MK, Liu ZR, Wang DY, Chang Q, Chen YB.** Alteration of somatostatin receptor subtype 2 gene expression in pancreatic tumor angiogenesis. *World J Gastroenterol* 2004; **10**: 132-135
- Caceres W, Gonzalez S.** Angiogenesis and cancer: recent advances. *P R Health Sci J* 2003; **22**: 149-151
- Shimamura M, Nagasawa H, Ashino H, Yamamoto Y, Hazato T, Uto Y, Hori H, Inayama S.** A novel hypoxia-dependent 2-nitroimidazole KIN-841 inhibits tumour-specific angiogenesis by blocking production of angiogenic factors. *Br J Cancer* 2003; **88**: 307-313
- Kieran MW, Billett A.** Antiangiogenesis therapy. Current and future agents. *Hematol Oncol Clin North Am* 2001; **15**: 835-851, viii
- Davis DW, McConkey DJ, Abbruzzese JL, Herbst RS.** Surrogate markers in antiangiogenesis clinical trials. *Br J Cancer* 2003; **89**: 8-14
- Hurwitz H, Fehrenbacher L, Novotny W, Cartwright T, Hainsworth J, Heim W, Berlin J, Baron A, Griffing S, Holmgren E, Ferrara N, Fyfe G, Rogers B, Ross R, Kabbinavar F.** Bevacizumab plus irinotecan, fluorouracil, and leucovorin for metastatic colorectal cancer. *N Engl J Med* 2004; **350**: 2335-2342
- Gragoudas ES, Adamis AP, Cunningham ET Jr, Feinsod M, Guyer DR.** Pegaptanib for neovascular age-related macular degeneration. *N Engl J Med* 2004; **351**: 2805-2816
- Cao Y, Cao R, Veitonmaki N.** Kringle structures and anti-angiogenesis. *Curr Med Chem Anticancer Agents* 2002; **2**: 667-681
- Magnon C, Galaup A, Mullan B, Rouffiac V, Bouquet C, Bidart JM, Griscelli F, Opolon P, Perricaudet M.** Canstatin acts on endothelial and tumor cells *via* mitochondrial damage initiated through interaction with alphavbeta3 and alphavbeta5 integrins. *Cancer Res* 2005; **65**: 4353-4361
- Wang QS, Yang X, Yang ZH, Gao GQ.** Novel method for expression and purification of human pigment epithelium-derived factor with biological activities in *Escherichia coli*. *Prep Biochem Biotechnol* 2006; **36**: 127-138
- Uchiyama T, Kawano H, Kusuhara Y.** The major outer membrane protein rOmpB of spotted fever group rickettsiae functions in the rickettsial adherence to and invasion of Vero cells. *Microbes Infect* 2006; **8**: 801-809

S- Editor Wang J L- Editor Zhu LH E- Editor Ma WH